




Chemical and microstructural characterization of three seaweed species from two locations of Veracruz, Mexico

Karina HERNÁNDEZ-CRUZ¹, Cristian JIMÉNEZ-MARTÍNEZ¹, Madeleine PERUCINI-AVENDAÑO¹,
Luz Elena MATEO CID², María de Jesús PEREA-FLORES³, Gustavo Fidel GUTIÉRREZ-LÓPEZ¹,
Gloria DÁVILA-ORTIZ^{1*} 

Abstract

Seaweeds or marine macroalgae are sources of industrial important macro compounds. This work characterizes the chemical composition, morphology, cellular structure, morphometric parameters, protein distribution, density, and quantifies the chemical elements of three seaweed species. The morphological characterization performed by Digital Image Analysis (DIA) showed that the length/width ratio for *UF* (*Ulva fasciata*) (15.4/10.9 cm) was greater compared to *SC* (*Sargassum cymosum*) and *GS* (*Grateloupia subpectinata*) (8.9/7.6 cm and 87/5.3 cm). Using Schiff's and Coomassie blue reagents, identified carbohydrates and proteins in cells and protein bodies (PB). Cell morphology showed larger cells in the SC cortex (457.8 μm^2) and smaller cells in the SC meristoderm (80.5 μm^2). PB density (PB/area) and distribution (area occupied by the cell, %) were higher in the cortex of *GS* (10468 PB/ mm^2 , 20%) and lower in the meristoderm of *SC* (917 PB/ mm^2 , 7%). Chemical analysis showed as major compounds: carbohydrates (12-46%), ashes (13-42%), and proteins (6-17%). Meanwhile, the concentration of metals was below the toxicity level. These results contribute to the knowledge of the structure-function relationship of seaweeds metabolites which could be a source of compounds of interest for the industrial sector.

Keywords: microscopy; histology; chemical composition; protein bodies; seaweeds.

Practical Application: Tissues seaweeds present interest macro compounds in food or biotechnology industry.

1 Introduction

Seaweeds are photosynthetic nonflowering plant-like organisms, divided into three major groups based on their dominant pigmentation: Chlorophyta or green algae, Rhodophyta, or red algae, and Ochrophyta that includes *Phaeophyceae* class or brown seaweed (Bonanno & Orlando-Bonaca, 2018). The macrostructure of seaweeds is like land plants, but the microstructure differs in the complexity of vascular tissues. Depending on the group, the morphological structure of algae consists of blades, e.g., *Ulva* genus (*Ulvales: Ulvaceae*), or thallus, e.g., *Sargassum* (*Fucales: Sargassaceae*) and *Grateloupia* (*Halymeniales: Halymeniaceae*). Such diversity is related to their chemical composition —determined by geographical and environmental conditions (Ak et al., 2021) — leading to the synthesis of compounds that participate in metabolic pathways: carbohydrates (ulvans, fucans, agarans, or carrageenans), enzymes (involved in photosynthesis; and synthesis of lipids, pigments, and amino acids) and minerals (P, K, Ca, S, Mn, Ni, Cu, Zn) (Harnedy & Fitz-Gerald, 2011; Wahlström et al., 2020).

Seaweed's cell wall comprises carbohydrates and proteins, which provide flexibility, resistance, and protection against

desiccation and other environmental adverse conditions (Harnedy & Fitz Gerald, 2011). Functional groups on cell walls surface —such as hydroxyl, carboxyl, sulfhydryl, and sulfate (negatively charged); and amino group (from polysaccharides, proteins, and lipids)— increase the ability of seaweed to uptake toxic metal ions, for example, heavy metal ions (Pb, Cd, Zn, Cu, Cr, and Ni) can bind to seaweed polysaccharides, and that provide them with a natural biosorption capacity (Barquilha et al., 2019; Bulgariu & Bulgariu, 2020), limiting their use for human or animal consumption.

Seaweed components (carbohydrates, protein, and metals) and morphology can be identified through different microscopy and histochemical techniques like optical microscopy (OM) and atomic absorption spectroscopy (AAS). Moreover, digital image analysis (DIA) may be a valuable tool for understanding the structure-functionality relationships based on microstructural features (Perea-Flores et al., 2011). This work aims to characterize three seaweed species through morphological parameters, cell structure identification, protein distribution and density and quantify the chemical elements to assess their toxicity potential.

Received 10 June, 2021

Accepted 21 Nov., 2021

¹Escuela Nacional de Ciencias Biológicas, Instituto Politécnico Nacional, México City, CdMx, México

²Departamento de Botánica, Escuela Nacional de Ciencias Biológicas, Instituto Politécnico Nacional, Miguel Hidalgo, CdMx, México

³Centro de Nanociencias y Micro y Nacional Nanotecnologías del Instituto Politécnico, Gustavo A. Madero, Ciudad de México, CDMX, México

*Corresponding author: gdavila@yahoo.com

2 Materials and methods

2.1 Biological material

Three samples of each seaweed species were collected in June 2018 in two locations. *Grateloupia subpectinata* (GS) was obtained from Tuxpan, Veracruz, Mexico (20°57'18" N, 97°23'59" W); *Sargassum cymosum* (SC) and *Ulva fasciata* (UF), were collected from "El Pulpo" beach in Barra de Cazones, Veracruz, Mexico (20°44'10" N, 97°11'38" W) and a record was made of the physicochemical parameters of the two zones (Table 1), pH of the water with potentiometer (Isolab), depth with Secchi disk, salinity by chemical test for chlorides (Hanna test kit, HI3835), ambient and seawater temperature with thermometer scale 1 to 100 °C and dissolved oxygen determination (Hanna HI-9146 kit). Seaweed samples were rinsed with seawater and distilled water to eliminate salts and epiphytes adhered to the thallus after they were placed in amber-colored flasks with a solution of NaCl (35 ppm), 10% ethanol, and distilled water to avoid decomposition (Florez-Leiva et al., 2010). The seaweeds were identified using taxonomic keys (Dawes & Mathieson, 2008) according to a phycological specialist at the herbarium of ENCB-IPN Mexico. Two samples were fixed in 2% glutaraldehyde with sodium cacodylate (1:1 v/v) and refrigerated until microscopy analysis. For the proximal chemical analysis, 1 kg of samples was dried at room temperature and grounded to a fine powder and was determined by following the AOAC standard procedures (Association of Official Analytical Chemists, 2019), moisture by method 925.09, protein by method 954.01, fat by method 920.39 and total dietary fiber by method 985.29, total carbohydrates were estimated by difference

2.2 Morphological and micro-structural characterization of seaweeds

Morphological evaluations of the three seaweed species (UF, SC, GS) were determined by measuring the length and width of the thallus and other structures: blades of UF, leaves of SC, and cylindrical branches of GS. Each specimen was photographed (13 MP 1:2.2/39 ASPH resolution) and the length/width ratio of each structure was measured with Image J version 1.52a software (NIH-2019, Bethesda, MD, USA). To evaluate the microstructure, samples were cut with a histological scalpel in sections depending on the species. Images were obtained by Optical Microscopy (MO) and Digital Image Analyses (DIA) through Image J 1.52a software (NIH, Bethesda, MD, USA).

Table 1. Physicochemical parameters of the collection zone.

Physicochemical parameters	Collection zone	
	Tuxpan beach	El Pulpo beach
pH	7.79 ± 0.20	8.80 ± 0.30
Depth (cm)	10.17 ± 0.02	19.30 ± 0.26
Salinity (g/kg)	19.63 ± 0.15	35.13 ± 0.02
Environmental temperature (°C)	24.06 ± 0.15	23.23 ± 0.58
Seawater temperature (°C)	23.60 ± 0.10	24.46 ± 0.58
Transparecy	90.00 ± 0.26	100 ± 0.001
Dissolved oxygen (mg/L)	7.13 ± 0.05	9.22 ± 0.07

Results were expressed as the mean value ± standard error.

2.3 Optical microscopy (OM)

The OM technique reported by Vicente-Flores et al. (2021) was used with some modifications. Firstly, four longitudinal sections and five cross-sections of seaweed species were acquired. Obtained the cuts from the apical blade section (UF), the apical leave section (SC), or the apical cylindrical branches section (GS). Additionally, were conducted a microstructural analysis (MAA) for the whole samples' area. The tissues were washed, dehydrated, cleared, and placed in Paraplast® I and II, and 10 µm thick histological sections were obtained with a microtome (RM 2235, Leica, Germany). The cut was deparaffinized and stained with Schiff's reagent and Coomassie Blue Brilliant (Monte-Domecq et al., 2003) to observe the presence of carbohydrates and protein. Captured brightfield images of each structure with an optical microscope (Eclipse 50i, Nikon, Tokyo, Japan).

Microstructural characterization through Digital Image Analysis

In the case of SC, PB were analyzed in meristoderm cells (A and B) located in two areas of the leaves: meristoderm A (PB distant from medulla cells) and meristoderm B (PB close to medulla cells). Determined morphometric parameters of the cells in different areas due to the structural differences of the blade, leaves, and cylindrical branches. Blade cells were evaluated in UF, meristoderm, cortex, and medulla cells in SC and cortex cells in GS. PB was evaluated in blade cells for UF, in meristoderm cells for SC, and in cortex cells for GS. Images of morphometric parameters and PB were obtained at 600 X magnification, and SC medulla cells were captured at 400 X magnification. Binary images were employed to obtain area (A), perimeter (P), Feret diameter (FD), roundness (R), and aspect ratio (AR) (Perea-Flores et al., 2011), also assessed area, distribution (percentage occupied by the PB in a specific area of the blades, leaves, or cylindrical branches), and density (number cells or PB by mm²) for PB.

2.4 Quantification of toxic metals

The toxic metals evaluation by Atomic Absorption Spectrometry (AAS; Perkin Elmer Analyst 100, USA), using the direct flame aspiration technique, according to Tapia-Martínez et al. (2019) method.

2.5 Statistical analyses

Statistical analysis was performed using Analysis of variance (ANOVA), followed by Tukey's multiple comparison test (Tukey's HSD, honestly significant difference) with MINITAB®17 software. All results are expressed as the mean value ± standard error.

3 Results and Discussion

3.1 Morphological and micro-structural description

Figure 1 describes the thallus structure of UF, SC, and GS. UF showed a brilliant green color, a blade (bla) like thallus, and a basal disk (di). The species' dimensions were 15.3 cm in length and 10.9 cm in width (Figure 1a). SC had a dark brown color, a

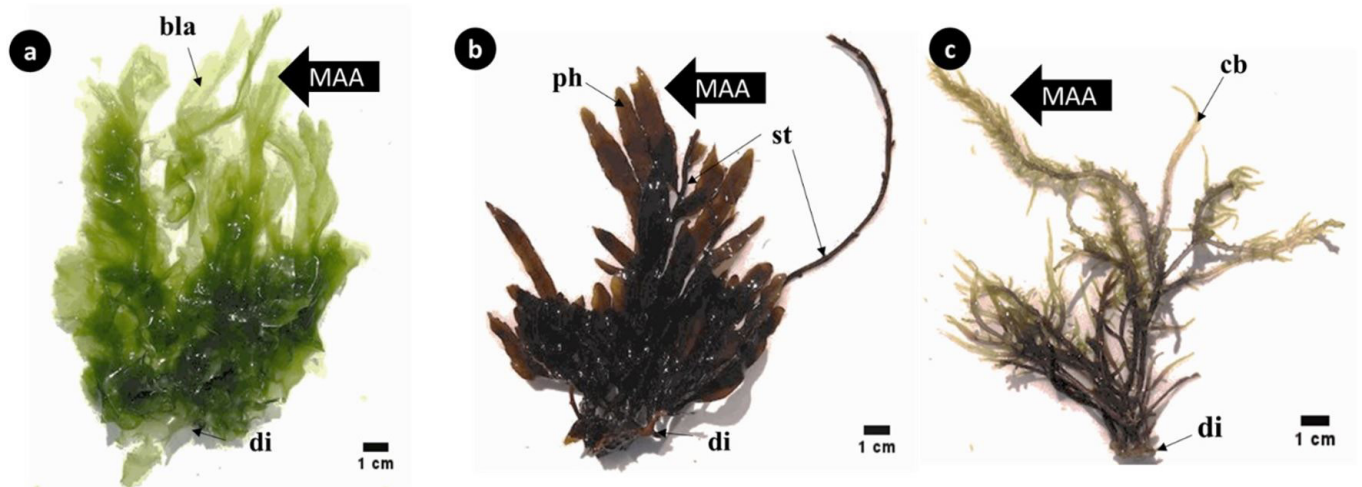


Figure 1. Scheme of the morphology general (thallus) (a) *U. fasciata* (green); (b) *S. cymosum* (brown); and (c) *G. subpectinata* (red). di: basal fixation disk; bla: blade; base; ph: leaves; st: stipe; cb: cylindrical branches; MAA: microstructural analysis area.

shrub-like thallus, and a basal disk (di) (Figure 1b). The collected species were 8.9 cm in length and 7.6 cm in width. These seaweeds presented stipes (st), one of their characteristic structures, and lateral branches alternated with elliptic, semi-rigid leaves (ph) with serrated borders and central midrib. *GS* had a reddish color with cylindrical, straight, and branched thalli, fixed through the basal disk (di) (Figure 1c). The species were 8.7 cm long and 5.3 cm wide; had cartilaginous, lax consistency; and bifurcated, opposite branching (1.1 cm long x 0.1 cm wide) and presented rounded and obtuse borders. Morphological structures revealed differences between the three species. The values obtained from the thalli of *UF*, *SC*, and *GS* showed significant differences ($p \leq 0.05$) (Table 2).

The largest thallus corresponded to *UF*, and the smallest to *GS*. However, *Sargassum* sp species can reach lengths of ≥ 200 cm (Guiry & Guiry, 2020). The morphological differences (Table 2) between the three seaweed species are associated with environmental conditions such as abiotic factors, high light intensity, temperature, and salinity (Lalegerie et al., 2020).

On the other hand, *UF* and *SC* grow in subtidal zones; hence, they are not exposed to low tide or extended periods of desiccation. *GS* grows in the intertidal zones, with alternating periods of emersion and immersion. The adverse environmental conditions (e.g., extended desiccation periods, solar radiation, osmotic changes, and nutrient limitation) induce adaptation and protection mechanisms in seaweeds that affect their growth (Kumar et al., 2014; Véliz et al., 2020).

Longitudinal and cross-section fields in different segments were observed to identify and describe the seaweeds microstructure (Figure 2). *UF* blade cells showed rectangular-square shapes in the transversal section (Figure 2b) and elongated or isodiametric forms in the longitudinal section (Figure 2d). Coomassie blue brilliant (CBB) staining method was used to visualize plastids (pl) in the seaweed cells. Within these organelles, pyrenoids were noticed; they form a dense structure inside chloroplasts

Table 2. Measurements of representative structures and thalli of algae of *UF*, *SC* and *GS*.

Size measure (cm)	Blade of <i>UF</i>	Leaves of <i>SC</i>	Cylindrical branches of <i>GS</i>
Length	15.4 ± 0.3 ^a	2.7 ± 0.1 ^b	1.1 ± 0.1 ^c
Width	0.9 ± 0.0 ^a	0.6 ± 0.0 ^b	0.1 ± 0.0 ^c
Global length thallus*	15.4 ± 0.3 ^a	8.9 ± 0.4 ^b	8.7 ± 0.4 ^b
Global width thallus*	10.9 ± 0.2 ^a	7.6 ± 0.4 ^b	5.3 ± 0.2 ^c

The results were expressed as the mean value ± standard error (n = 20). *In the row, different letters indicate statistical differences ($p < 0.05$) between the thalli of the three species studied. *UF*: *U. fasciata*; *SC*: *S. cymosum*; *GS*: *G. subpectinata*.

of certain green seaweeds, which contain Ribulose biphosphate carboxylase, an enzyme that participates in photosynthesis (Meyer et al., 2020). Lastly, cell walls (cw) stained in magenta (Figure 2d) due to carbohydrate composition (Schiff reagent stain) were identified.

SC leaves (ph) in the cross, and longitudinal sections are composed of three layers: meristoderm cells (mer) arranged on the periphery (as an epidermis), parenchyma (cortex cells) (cor), and compact-elongated medulla cells (med) (midrib) at the central zone (Figures 2e, 2g). The stipe (st) consists of several layers of cortex cells surrounded by a layer of meristoderm cells. The (cor) cells are separated by a large cell space, which allows the algae to float on the sea surface (Mateluna et al., 2020).

Cross and longitudinal sections (Figures 2m and 2o) obtained from *GS* cylindrical branches are composed of cortex cells (cor), star-shaped cells in the subcortex (scor), and filamentous medulla (fm) cells. Stained cell walls (cw) of *UF* seaweed (Figure 2d) correspond to sulfated polysaccharides, e.g., ulvans reported for *Ulva* sp (Stiger-Pouvreau et al., 2016). Figures 2f and 2h show longitudinal and cross-sections of *SC* (ph), where different structures (meri, cor, and med) are evidenced by cell wall staining. In this respect, Vijay et al. (2017) reported that cells carbohydrates of the *Sargassum* genus are constituted by fucoidan, laminaran, cellulose, and alginate,

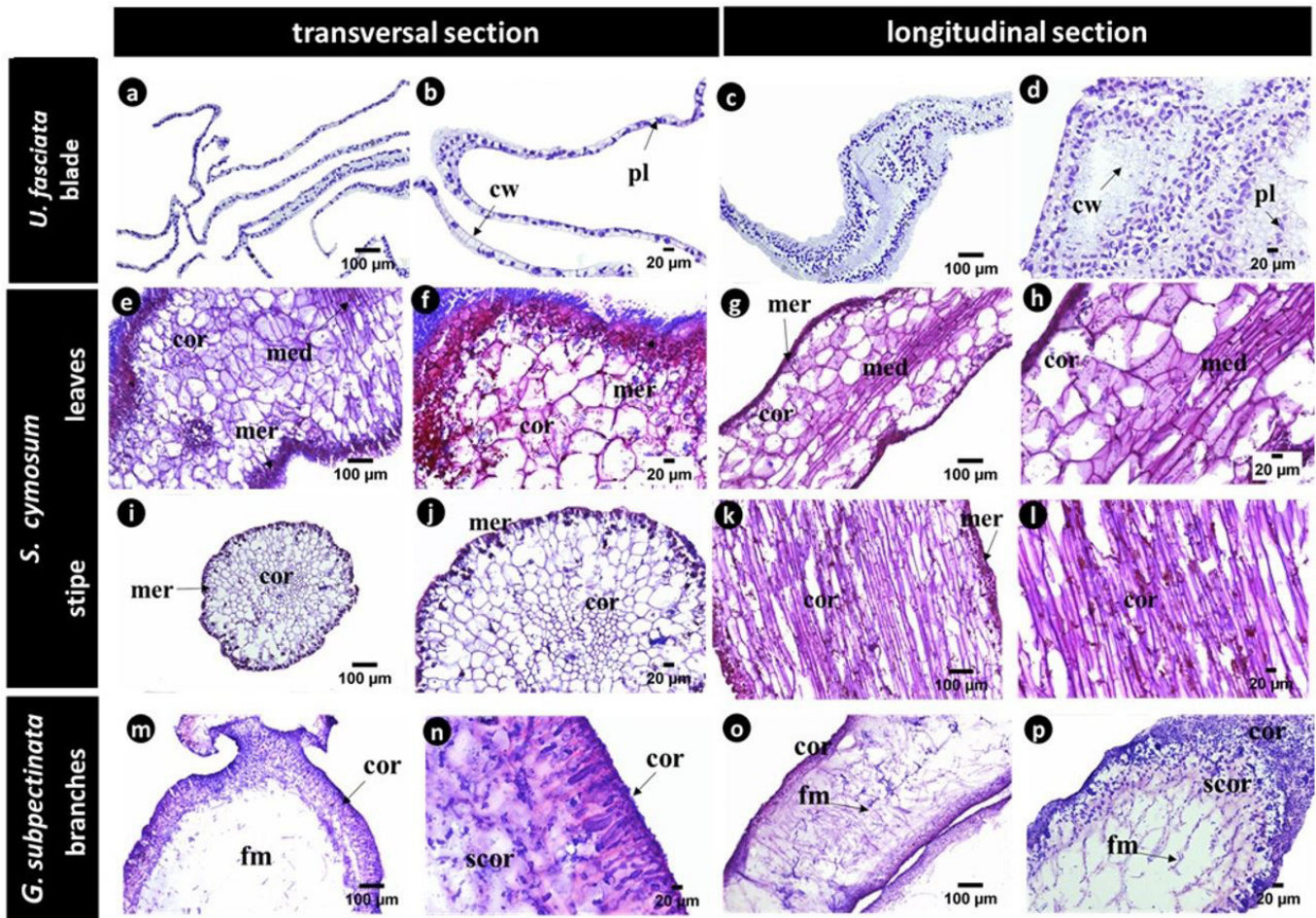


Figure 2. Scheme of the general microstructure of the *U. fasciata* blade, leaves and stipe of *S. cymosum*, and cylindrical branches of *G. subpectinata*. Transversal and longitudinal sections 10X (a, c, e, g, i, k, m, o) y 20X (b, d, f, h, j, l, n, p); cw: cell wall; pl: plastids; mer: meristoderm; cor: cortex; scor: subcortex; med: medulla; fm: filamentous medulla

Figures 2n and 2p display the carbohydrate composition of (cor) and (scor) cells obtained from GS. According to Sen et al. (1994), *G. indica* exhibits galactose units that form homoglycans. Complex carbohydrates in cell walls contribute to algae resistance and flexibility (Khora & Navya, 2020), regulate the ionic balance of the internal cells to prevent desiccation (O'Sullivan et al., 2010), and stimulate the synthesis of enzymes involved in metabolism. According to Lalegerie et al. (2020), carbohydrates are also associated with adaptation mechanisms.

Figure 2 shows blue-stained PB, resulting from the reaction between the triphenylmethane functional groups of the CBB colorant and the protein nitrogenated group. PB are synthesized from inorganic nitrogen compounds present in seawater (Yanagisawa, 2014). In *UF*, PB was mainly identified in blade cells' chloroplasts (Figure 2b, 2d), related to catalytic proteins — located in thylakoid membranes or stored in vacuoles—that participate in photosynthesis (Trösch et al., 2018).

A cross-section image from SC (ph) shows the PB from meristoderm (Figure 2e). The (mer) segment closest to the medulla (mer B) exhibits higher PB accumulation (Figure 2f)

in contrast to distant (mer A) (Figure 2f). *GS* transversal section of the cylindrical branch (Figure 2m) indicates a higher PB concentration at cortex and subcortex cells (Figure 2n, 2p).

PB are mainly located in the chloroplast, cell wall, and cytosol. Algae proteins act as a reserve for growth and have protection-defense activities (lectins) (Harnedy & Fitz Gerald, 2011). Conversely, López-Cristoffanini et al. (2015) reported catalytic proteins involved in energy metabolism, defense-antioxidants functions, environmental-genetic protection, and transportation, and it identified cytoskeleton-related proteins in red algae (92%) and other species (less than 2%).

3.2 Microstructural analysis of cells and protein bodies (PB)

The microstructural analysis revealed that the largest cells are located at SC (cor) (A: 457.8 μm^2) (Figure 3e), whereas the smallest ones are at the meristoderm (80.5 μm^2) (Figure 3e). SC (cor) cell area (457.8 μm^2) was five times higher than GS area (399.3 μm^2) (Figures 3e, 3l). *UF* blade cells (Figure 3b) comprise an area of 163.4 μm^2 (Table 3). SC (med) cells presented a greater perimeter (100.2 μm) than meristoderm cells (36.4 μm) (Table 3).

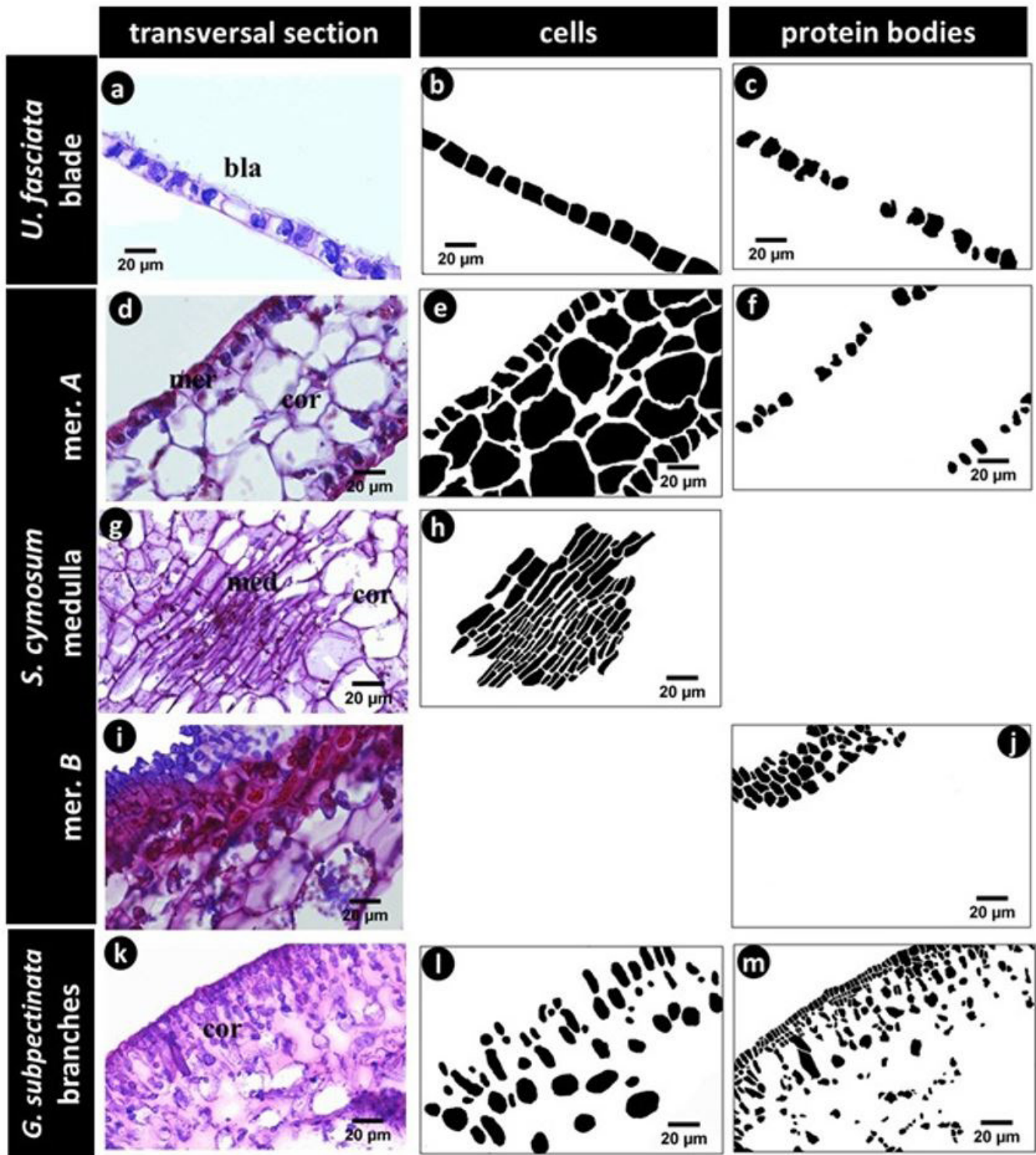


Figure 3. Transversal section (60X) of the blade, leaves, and cylindrical branches. Optical images (a, d, g, i, k) (stained with Schiff and Coomassie blue); segmented images of cells (b, e, h, l) and protein bodies (c, f, j, m). In *UF* (blade) there are blade cells, in *SC* (leaves), there are meristoderm (mer) and figure (d) refers to mer. Figure (i); refers mer; (B), cortex (cor), and medulla (med) cells, and *GS*, (branches) there are cortex cells (cor).

GS (cor) cells showed a similar perimeter (37.7 μm) to *SC* (mer) cells, while *UF* (bla) cells had larger perimeters (52.6 μm) than *GS* (cor) cells and *SC* (mer) cells. Based on the morphometric parameters of aspect ratio (AR) and roundness (R), the cells of

SC medulla are more elongated (AR:4.0, R:0.3) than those of the (mer) (AR:1.7, R:0.6) and the (cor) (AR:1.8, R:0.6). *GS* cells were similar in shape (AR:1.7, R:0.6). Rounder cells were found in *UF* (bla) (AR:1.4, R:0.8).

Table 3. Morphometric parameters of cells and protein bodies (PB) in transversal sections of the seaweed studied.

Cellular morphometric parameters*	UF		SC		GS
	Blade	Meristoderm	Cortex	Medulla	Cortex
A (μm^2)	163.4 \pm 7.8	80.5 \pm 4.5	457.8 \pm 36.7	399.3 \pm 25.4	97.0 \pm 6.3
P (μm)	52.6 \pm 1.4	36.4 \pm 1.0	89.2 \pm 3.8	100.2 \pm 3.4	37.7 \pm 1.2
FD (μm)	18.2 \pm 0.5	13.0 \pm 0.4	31.7 \pm 1.3	41.4 \pm 1.5	13.6 \pm 0.4
AR	1.4 \pm 0.0	1.7 \pm 0.0	1.8 \pm 0.0	4.0 \pm 0.1	1.7 \pm 0.0
R	0.8 \pm 0.0	0.6 \pm 0.0	0.6 \pm 0.0	0.3 \pm 0.0	0.6 \pm 0.0
Protein bodies (PB)*	Blade	Meristoderm A	Meristoderm B	Cortex	
A (μm^2)	93.5 \pm 5.53	71.1 \pm 37.0	45.5 \pm 22.4	19.7 \pm 0.6	
Distribution (%)	32 \pm 9.5	7 \pm 2.0	14 \pm 10.1	20 \pm 4.0	
Density (PB/mm ²)	3 083 \pm 769	917 \pm 163	2 969 \pm 2078	10 468 \pm 1805	

*Results were expressed as the mean value \pm standard error (n=3); A: area; P: Perimeter; FD: Feret diameter; AR: Aspect ratio; R: Roundness. UF: *U. fasciata*; SC: *S. cymosum*; GS: *G. subpectinata*. In case of SC for Meristoderm A refers to distant al medulla cells and Meristoderm B refers to near at medulla cells.

Image analyses revealed that PB in the UF (bla) cells had a larger area (93.5 μm^2) than GS (cor) cells (19.7 μm^2). According to these values, PB distribution was 32% inside UF (bla) cells, 20% in GS cortex cells, 14% in SC (mer) B, and 7% in SC (mer) A. Table 3 shows the PB density values of the three seaweed species, dependent on their size ranging from 19.7 μm^2 to 93.5 μm^2 . Density values were 10468 PB/mm² for GS, 3083 PB/mm² for UF, 2969 PB/mm² for SC (mer) B, and 917 PB/mm² for SC (mer) A.

The image analysis allowed us to find differences in PB area, distribution, and density in the three seaweed species cells. Variations could be related to cell differentiation processes, regulated by enzymes such as nitrate-reductase (Yanagisawa, 2014) involved in the assimilation of inorganic nitrogen compounds by reducing nitrates to nitrites for protein synthesis. PB plays a fundamental role in seaweed metabolism. The quantification of the area, distribution, and density of those compounds in the cell contribute to understanding their potential function in different algae tissues (UF blade, SC leaves, and GS cylindrical branches).

3.3 Chemical proximal analyses

Table 4 shows the results from the proximate chemical analysis for the three studied seaweeds. Moisture content was lower than 13.7 g/100 g on a dry basis for all species. Moisture values below 10% are adequate to avoid microbial decomposition (Di Filippo-Herrera et al., 2018). Total carbohydrate content was variable. The carbohydrate content ranges between 12 in SC and 45 g/100 g in UF and SC. Nevertheless, previous research declared 35–49% values in different algae (Di-Filippo-Herrera et al., 2018; El-Sheekh et al., 2021; El Zokm et al., 2021). Regarding ash content, a higher concentration was found in SC (42 g/100 g), followed by GS (20.2 g/100 g) and UF (12.9 g/100 g). Ash content among seaweed species varies between 20–25 g/100 g (Di-Filippo-Herrera et al., 2018; Tapia-Martínez et al., 2019). Kumar et al. (2014) attributed these differences to growing area and harvesting season.

Protein content varied between 5.9 and 16.9 g/100 g. The protein content of UF is within the stated values (4 to 15.9 g/100 g) for this species (Pirian et al., 2016; Ismail, 2017). SC presented a lower protein content than other *Sargassum* species, e.g., 9, 6.5, and 10.3 g/100 g for *S. cymosum*, *S. horridum*, *S. liebmanni*,

respectively (Rubio et al., 2017; Di Filippo-Herrera et al., 2018; Tapia-Martínez et al., 2019). For GS, protein value was close to the *G. turuturu* species, 22.5 g/100 g (Rodrigues et al., 2015).

Regarding fiber content, UF had 28.2 g/100 g, consistent with Rasyid (2017) analysis. SC contained 35.1 g/100 g of fiber, in contrast to *S. wightii* that showed a higher ratio (53.52 g/100 g) (Praveen et al., 2019). GS fiber content was lower than *G. turuturu* (53.06 to 61.28 g/100 g) (Denis et al., 2010). Lipids represented less than 6% of the total weight of seaweeds. UF presented a concentration of 4.4 and SC, 4.5 g/100 g, showing a significant difference compared to GS ($p < 0.05$). Studies reported that *U. lactuca* lipid content ranges from 0.56 to 0.85 g/100 g (Pirian et al., 2016). Brown seaweed species contain 1.45 to 2.20 g/100 g (Rodrigues et al., 2015). Seaweed lipids are a source of EPA (eicosapentaenoic acid), DHA (docosahexaenoic acid), and ARA (arachidonic acid), essential compounds for human health (Harwood, 2019).

Results obtained by AAS are presented in Table 4. The lowest values of metals considered toxic (Ak et al., 2021) were Hg 0.001–0.01 $\mu\text{g/g}$ and Cd 0.01–0.06 $\mu\text{g/g}$. While the higher values for UF were Ni 0.51 $\mu\text{g/g}$; for SC, Zn 0.96 $\mu\text{g/g}$; and for GS, Cu 1.48 $\mu\text{g/g}$. Greater concentrations of toxic metals in edible brown algae have been reported: Cd 0.82 $\mu\text{g/g}$, Cr 0.04 $\mu\text{g/g}$, and Pb 0.02 $\mu\text{g/g}$; Hg 1.2–2.4 $\mu\text{g/g}$, and Pb 5 $\mu\text{g/g}$ (Paz et al., 2019; Rubio et al., 2017). The concentration of toxic metals in the studied algae species was below the permissible levels for human consumption like Cd (0.01, 0.06 and 0.06), Pb (0.17, 0.75, and 0.65), and Hg (< 0.001), for UF, SC, and GS respectively (Agence Française de Sécurité Sanitaire des Aliments, 2009; Agency for Toxic Substances and Disease Registry, 2021).

The high concentration of metals in some seaweed species is related to anthropogenic and industrial activities and environmental conditions that impact the biosorption capacity of algae (Chalkley et al., 2019; Paz et al., 2019). However, the metal content in seaweeds depends on the collection zone (Paz et al., 2019). Frequent consumption of seaweeds may benefit to human health, e.g., diabetes, cholesterol, heart disease, lipid lowering, cancer and others (Kumar & Sharma, 2021).

Table 4. Proximal chemical analysis and quantify metals of *UF*, *SC*, and *GS*.

Components	UF	SC	GS	Permissible limits**
Moisture	13.7 ± 0.2 ^a	6.0 ± 0.2 ^c	9.6 ± 0.1 ^b	--
Total carbohydrates*	45.9 ± 1.4 ^a	12.3 ± 1.1 ^c	45.1 ± 0.5 ^a	--
Dietary fiber*	28.2 ± 0.9 ^b	35.1 ± 0.5 ^a	22.4 ± 0.2 ^c	--
Proteins*	8.5 ± 0.0 ^b	5.9 ± 0.1 ^c	16.9 ± 0.0 ^a	--
Lipids*	4.5 ± 0.03 ^{ab}	4.5 ± 0.1 ^a	5.3 ± 0.5 ^b	--
Ashes*	12.9 ± 1.5 ^c	42.1 ± 0.0 ^a	20.2 ± 0.1 ^b	--
Metals¹				µg / g
Cu	0.27 ± 0.001 ^a	0.90 ± 0.000 ^b	1.48 ± 0.001 ^c	<1000 ^B
Cd	0.01 ± 0.001 ^c	0.06 ± 0.001 ^a	0.06 ± 0.001 ^b	<0.5 ^A
Cr	0.42 ± 0.001 ^a	0.20 ± 0.001 ^c	0.21 ± 0.000 ^b	< 100 ^B
Ni	0.51 ± 0.001 ^a	0.50 ± 0.001 ^b	0.46 ± 0.000 ^c	< 1 ^B
Pb	0.17 ± 0.001 ^c	0.75 ± 0.002 ^a	0.65 ± 0.013 ^b	<5 ^A
Zn	0.32 ± 0.001 ^c	0.96 ± 0.000 ^a	0.76 ± 0.001 ^b	<5000 ^B
Hg	0.001 ± 0.000 ^b	0.01 ± 0.000 ^a	0.01 ± 0.000 ^a	<0.1 ^A

*g/100 g dry base; ¹µg/g. Results were expressed as the mean value ± standard error (n=3); In the row, different letters indicate statistical differences ($p < 0.05$) between the thalli of the three species studied. **Agence Française de Sécurité Sanitaire des Aliments (2009)^a; Agency for Toxic Substances and Disease Registry (2021)^b.

4 Conclusions

The chemical, morphological and microstructural characterization of three seaweeds species from the state of Veracruz, Mexico, allowed us to identify some major components of the blades, leaves, and cylindrical branches, such as proteins and carbohydrates. In addition, certain toxic elements were found at low concentration levels through quantitative chemical analyses. These results contribute to the knowledge of the structure-function relationship of the seaweed tissues, considered as a potential source of various metabolites that could be used in the food, pharmaceutical, and cosmetic industries.

Acknowledgements

This study was financially supported by the Instituto Politécnico Nacional, Mexico (SIP projects: 20200291, 20200299 and 20180489). Authors are grateful to CONACyT (Mexico) for the support provided through study grants, and to CIEMAD-IPN for the technical assistance offered.

References

- Agence Française de Sécurité Sanitaire des Aliments – AFSSA. (2009). *Avis de l'Agence Française de Sécurité Sanitaire des Aliments relatif à la teneur maximale en arsenic inorganique recommandée pour les algues laminaires et aux modalités de consommation de ces algues compte tenu de leur teneur élevée en iode*. France. Retrieved from <https://www.anses.fr/fr>
- Agency for Toxic Substances and Disease Registry – ATSDR. (2021). *Public health service: toxicological profiles*. Retrieved from <https://www.atsdr.cdc.gov/>
- Ak, İ., Çankiriligil, E. C., Türker, G., & Sever, O. (2021). Assessment of light intensity and salinity regimes on the element levels of brown macroalgae, *Treptacantha barbata*: application of response surface methodology (RSM). *Food Science and Technology*, 41(4), 944-952. <http://dx.doi.org/10.1590/fst.25220>
- Association of Official Analytical Chemists – AOAC. (2019). *Official methods of analysis* (21st ed.). Arlington: EEUU.
- Barquilha, C. E., Cossich, E. S., Tavares, C. R., & Silva, E. A. (2019). Biosorption of nickel (II) and copper (II) ions from synthetic and real effluents by alginate-based biosorbent produced from seaweed *Sargassum* sp. *Environmental Science and Pollution Research International*, 26(11), 11100-11112. <http://dx.doi.org/10.1007/s11356-019-04552-0>. PMID:30788702.
- Bonanno, G., & Orlando-Bonaca, M. (2018). Chemical elements in Mediterranean macroalgae: a review. *Ecotoxicology and Environmental Safety*, 148, 44-71. <http://dx.doi.org/10.1016/j.ecoenv.2017.10.013>. PMID:29031118.
- Bulgariu, L., & Bulgariu, D. (2020). New alternative fertilizers based on algae biomass loaded with metal ions. In K. Se-Kwon (Ed.), *Encyclopedia of marine biotechnology* (Chap. 17, pp. 515-546). USA: John Wiley & Sons. <http://dx.doi.org/10.1002/9781119143802.ch17>.
- Chalkley, R., Child, F., Al-Thaqafi, K., Dean, A. P., White, K. N., & Pittman, J. K. (2019). Macroalgae as spatial and temporal bioindicators of coastal metal pollution following remediation and diversion of acid mine drainage. *Ecotoxicology and environmental safety*, 182, 109458. <https://doi.org/10.1016/j.ecoenv.2019.109458>.
- Dawes, C. J., & Mathieson, A. C. (Ed.). (2008). *The seaweeds of Florida*. Gainesville: University Press of Florida.
- Denis, C., Morançais, M., Li, M., Deniaud, E., Gaudin, P., Wielgosz-Collin, G., Barnathan, G., Jaouen, P., & Fleurence, J. (2010). Study of the chemical composition of edible red macroalgae *Grateloupia turuturu* from Brittany (France). *Food Chemistry*, 119(3), 913-917. <http://dx.doi.org/10.1016/j.foodchem.2009.07.047>.
- Di Filippo-Herrera, D. A., Hernández-Carmona, G., Muñoz-Ochoa, M., Arvizu-Higuera, D. L., & Rodríguez-Montesinos, Y. E. (2018). Monthly variation in the chemical composition and biological activity of *Sargassum horridum*. *Botanica Marina*, 61(1), 91-102. <http://dx.doi.org/10.1515/bot-2017-0031>.
- El Zokm, G. M., Ismail, M. M., & El-Said, G. F. (2021). Halogen content relative to the chemical and biochemical composition of fifteen marine macro and micro algae: nutritional value, energy supply, antioxidant potency, and health risk assessment. *Environmental*

- Science and Pollution Research International*, 28(12), 14893-14908. <http://dx.doi.org/10.1007/s11356-020-11596-0>. PMID:33222067.
- El-Sheekh, M. M., El-Shenody, R. A. E. K., Bases, E. A., & El Shafay, S. M. (2021). Comparative assessment of antioxidant activity and biochemical composition of four seaweeds, rocky bay of abu qir in Alexandria, Egypt. *Food Science and Technology*, 41(1, Suppl. 1), 29-40. <http://dx.doi.org/10.1590/fst.06120>.
- Florez-Leiva, L., Gavio, B., Díaz-Ruíz, M., & Camacho, O. (2010). Recolección y preservación de macroalgas marinas: una guía para estudios ficológicos. *Revista Intropica*, 5, 5-11.
- Guiry, M. D., & Guiry, G. M. (2020). *AlgaeBase*. Galway: National University of Ireland. Retrieved from <http://www.algaebase.org>
- Harnedy, P. A., & FitzGerald, R. J. (2011). Bioactive proteins, peptides, and amino acids from macroalgae. *Journal of Phycology*, 47(2), 218-232. <http://dx.doi.org/10.1111/j.1529-8817.2011.00969.x>. PMID:27021854.
- Harwood, J. L. (2019). Algae: critical sources of very long-chain polyunsaturated fatty acids. *Biomolecules*, 9(11), 1-14. <http://dx.doi.org/10.3390/biom9110708>. PMID:31698772.
- Ismail, G. A. (2017). Biochemical composition of some Egyptian seaweeds with potent nutritive and antioxidant properties. *Food Science and Technology*, 37(2), 294-302. <http://dx.doi.org/10.1590/1678-457x.20316>.
- Khora, S. S., & Navya, P. (2020). Bioactive polysaccharides from marine macroalgae. In S.-K. Kim (Ed.), *Encyclopedia of marine biotechnology* (pp. 121-145). Hoboken: Wiley-Blackwell. <http://doi.org/10.1002/9781119143802.ch6>.
- Kumar, M. S., & Sharma, S. A. (2021). Toxicological effects of marine seaweeds: a cautious insight for human consumption. *Critical Reviews in Food Science and Nutrition*, 61(3), 500-521. <http://dx.doi.org/10.1080/10408398.2020.1738334>. PMID:32188262.
- Kumar, M., Kumari, P., Reddy, C. R. K., & Jha, B. (2014). Salinity and desiccation induced oxidative stress acclimation in seaweeds. In N. Bourgougnon (Ed.), *Advances in botanical research* (Chap. 4, pp. 91-123). Massachuset: Academic Press-Elsevier.
- Lalegerie, F., Gager, L., Stiger-Pouvreau, V., & Connan, S. (2020). The stressful life of red and brown seaweeds on the temperate intertidal zone: effect of abiotic and biotic parameters on the physiology of macroalgae and content variability of particular metabolites. In N. Bourgougnon (Ed.), *Advances in botanical research* (Chap. 8, pp. 247-287). Massachuset: Academic Press-Elsevier. <http://doi.org/10.1016/bs.abr.2019.11.007>.
- López-Cristoffanini, C., Zapata, J., Gaillard, F., Potin, P., Correa, J. A., & Contreras-Porcia, L. (2015). Identification of proteins involved in desiccation tolerance in the red seaweed *Pyropia orbicularis* (Rhodophyta, Bangiales). *Proteomics*, 15(23-24), 3954-3968. <http://dx.doi.org/10.1002/pmic.201400625>. PMID:26154304.
- Mateluna, C., Figueroa, V., Ortiz, J., & Aguilera, J. M. (2020). Effect of processing on texture and microstructure of the seaweed *Durvillaea antarctica*. *Journal of Applied Phycology*, 32(6), 4211-4219. <http://dx.doi.org/10.1007/s10811-020-02259-1>.
- Meyer, M. T., Goudet, M. M. M., & Griffiths, H. (2020). The Algal Pyrenoid. In A. Grossman, J. Raven & A. Larkum (Eds.), *Photosynthesis in Algae: biochemical and physiological mechanisms* (Advances in Photosynthesis and Respiration, Chap. 45, pp. 179-203). Cham: Springer. http://dx.doi.org/10.1007/978-3-030-33397-3_9.
- Monte-Domecq, F. A., Ouriques, L. C., & Bouzon, Z. L. (2003). Tetrasporogenesis in *Gelidium floridanum* (GELIDIALES, RHODOPHYTA): Cytochemical study. *Acta Microscopica*, 12, 21-22.
- O'Sullivan, L., Murphy, B., McLoughlin, P., Duggan, P., Lawlor, P. G., Hughes, H., & Gardiner, G. E. (2010). Prebiotics from Marine macroalgae for human and animal health applications. *Marine Drugs*, 8(7), 2038-2064. <http://dx.doi.org/10.3390/md8072038>. PMID:20714423.
- Perea-Flores, M. J., Chanona-Pérez, J. J., Garibay-Febles, V., Calderón-Dominguez, G., Terrés-Rojas, E., Mendoza-Pérez, J. A., & Herrera-Bucio, R. (2011). Microscopy techniques and image analysis for evaluation of some chemical and physical properties and morphological features for seeds of the castor oil plant (*Ricinus communis*). *Industrial Crops and Products*, 34(1), 1057-1065. <http://dx.doi.org/10.1016/j.indcrop.2011.03.015>.
- Pirian, K., Piri, K., Sohrabipour, J., Jahromi, S., & Blomster, J. (2016). Nutritional and phytochemical evaluation of the common green algae, *Ulva* spp. (Ulvophyceae), from the Persian Gulf. *Fundamental and Applied Limnology*, 188(4), 315-327. <http://dx.doi.org/10.1127/fal/2016/0947>.
- Paz, S., Rubio, C., Frías, I., Gutiérrez, Á. J., González-Weller, D., Martín, V., Revert, C., & Hardisson, A. (2019). Toxic metals (Al, Cd, Pb and Hg) in the most consumed edible seaweeds in Europe. *Chemosphere*, 218, 879-884. <http://dx.doi.org/10.1016/j.chemosphere.2018.11.165>. PMID:30609492.
- Praveen, M. A., Parvathy, K. K., Jayabalan, R., & Balasubramanian, P. (2019). Dietary fiber from Indian edible seaweeds and its in-vitro prebiotic effect on the gut microbiota. *Food Hydrocolloids*, 96, 343-353. <http://dx.doi.org/10.1016/j.foodhyd.2019.05.031>.
- Rasyid, A. (2017). Evaluation of nutritional composition of the dried seaweed *Ulva lactuca* from Pameungpeuk waters, Indonesia. *Tropical Life Sciences Research*, 28(2), 119-125. <http://dx.doi.org/10.21315/tlsr2017.28.2.9>. PMID:28890765.
- Rodrigues, D., Freitas, A. C., Pereira, L., Rocha-Santos, T. A., Vasconcelos, M. W., Roriz, M., Rodríguez-Alcalá, L. M., Gomes, A. M., & Duarte, A. C. (2015). Chemical composition of red, brown and green macroalgae from Buarcos bay in Central West Coast of Portugal. *Food Chemistry*, 183, 197-207. <http://dx.doi.org/10.1016/j.foodchem.2015.03.057>. PMID:25863629.
- Rubio, C., Napoleone, G., Luis-González, G., Gutiérrez, A. J., González-Weller, D., Hardisson, A., & Revert, C. (2017). Metals in edible seaweed. *Chemosphere*, 173, 572-579. <http://dx.doi.org/10.1016/j.chemosphere.2017.01.064>. PMID:28152409.
- Sen, A. K., Sr., Da, A. K., Banerji, N., Siddhanta, K. H., Mody, K. H., Ramavat, B. K., Chauhan, V. D., Vedasiromoni, J. R., & Ganguly, D. K. (1994). A new sulfated polysaccharide with potent boole anti-coagulant activity from the red seaweed *Grateloupia indica*. *International Journal of Biological Macromolecules*, 16(5), 279-280. [http://dx.doi.org/10.1016/0141-8130\(94\)90034-5](http://dx.doi.org/10.1016/0141-8130(94)90034-5). PMID:7893632.
- Stiger-Pouvreau, V., Bourgougnon, N., & Deslandes, E. (2016). Carbohydrates from Seaweeds. In J. Fleurence & I. Levine (Eds.), *Seaweed health and disease prevention* (Chap. 8, pp. 223-274). Cambridge: Academic Press-Elsevier. <http://dx.doi.org/10.1016/B978-0-12-802772-1.00008-7>.
- Tapia-Martínez, J., Hernández-Cruz, K., Franco-Colín, M., Mateo-Cid, L. E., Mendoza-Gonzalez, A. C., Blas-Valdivia, V., & Cano-Europa, E. (2019). Safety evaluation and antiobesogenic effect of *Sargassum liebmannii* J. Agardh (Fucales: *Phaeophyceae*) in rodents. *Journal of Applied Phycology*, 31(4), 2597-2607. <http://dx.doi.org/10.1007/s10811-019-1752-y>.
- Trösch, R., Barahimipour, R., Gao, Y., Badillo-Corona, J. A., Gotsmann, V. L., Zimmer, D., Mühlhaus, T., Zoschke, R., & Willmund, F. (2018). Commonalities and differences of chloroplast translation in a green

- alga and land plants. *Nature Plants*, 4(8), 564-575. <http://dx.doi.org/10.1038/s41477-018-0211-0>. PMID:30061751.
- Véliz, K., Chandia, N., Bischof, K., & Thiel, M. (2020). Geographic variation of UV stress tolerance in red seaweeds does not scale with latitude along the SE Pacific coast. *Journal of Phycology*, 56(4), 1090-1102. <http://dx.doi.org/10.1111/jpy.13009>. PMID:32348548.
- Vicente-Flores, M., Güemes-Vera, N., Chanona-Pérez, J. J., Perea-Flores, M. D. J., Arzate-Vázquez, I., Quintero-Lira, A., & Sánchez-Fuentes, C. E. (2021). Study of cellular architecture and micromechanical properties of cuajilote fruits (*Parmentiera edulis* DC) using different microscopy techniques. *Microscopy Research and Technique*, 84(1), 12-27. <http://dx.doi.org/10.1012/jemt.23559>. PMID:32905658.
- Vijay, K., Balasundari, S., Jeyashakila, R., Velayathum, P., Masilan, K., & Reshma, R. (2017). Proximate and mineral composition of brown seaweed from Gulf of Mannar. *International Journal of Fisheries and Aquatic Studies*, 5(5), 106-112.
- Wahlström, N., Nylander, F., Malmhäll-Bah, E., Sjökvold, K., Edlund, U., Westman, G., & Albers, E. (2020). Composition and structure of cell wall ulvans recovered from *Ulva* spp. along the Swedish west coast. *Carbohydrate Polymers*, 233, 115852. <http://dx.doi.org/10.1016/j.carbpol.2020.115852>. PMID:32059903.
- Yanagisawa, S. (2014). Transcription factors involved in controlling the expression of nitrate reductase genes in higher plants. *Plant Science*, 229, 167-171. <http://dx.doi.org/10.1016/j.plantsci.2014.09.006>. PMID:25443843.